Effect of Femtosecond-laser Irradiation on Magnetic and Optical Properties in Au- and Fe-doped Transparent Glass

Seisuke NAKASHIMA[*1, *2], Koji SUGIOKA[*1], Katsumi MIDORIKAWA[*1], and Kohki MUKAI[*2]

[*1] *Advanced Science Institute, RIKEN, 2-1 Hirosawa, Wako, Saitama 351-0198, Japan*
E-mail: nakashima@ynu.ac.jp
[*2] *Yokohama National University, 79-5 Tokiwadai, Hodogaya-ku, Yokohama-shi, Kanagawa 240-8501, Japan*

We have investigated an effect of near-infrared femtosecond- (fs-) laser irradiation on magnetic and optical properties in Au- and Fe-doped transparent glasses. A fs-laser beam with a wavelength of 775 nm was focused 1 mm below the surfaces of glass samples. This produces absorption peaks due to the formation of hole-trap centers in the irradiated region, which changes into different peaks originated from localized surface plasmon absorption after annealing at 450°C. It is presumed that precipitation of Au nanoparticles occurs as results of photoreduction of Au ions and agglomeration by the thermal atomic diffusion. In addition, enhancement of magnetization in the localized area inside the glass was realized after laser irradiation and subsequent annealing. Ferrimagnetic behaviors were increased in the *M-H* curve even at room temperature, whereas the diamagnetic component dominated in the *M-H* curve of the as-prepared glass sample. The irradiated and annealed glass sample also exhibited superparamagnetic blocking in the temperature dependence of the magnetization with a blocking temperature higher than room temperature. These changes in magnetic properties are explainable in terms of the local crystallization of ferrimagnetic nanoparticles, such as magnetite, induced by fs-laser irradiation and annealing. Transmission-electron-microscopy observations support our considerations that Au nanoparticles and ferrimagnetic spinel-phase nanoparticles were simultaneously and separately crystallized in the focused region of the fs-laser beam.
DOI:10.2961/jlmn.2012.02.0015

Keywords: Femtosecond laser, Ferrimagnetic nanoparticle, Superparamagnet, Plasmonic material, Localized surface plasmon resonance

1. Introduction

Ultrashort-pulse-laser induced synthesis of nanocrystalline materials in transparent glasses has attracted considerable attention for its potential applications in a variety of devices, such as nonlinear optical devices, plasmonic devices, and magnetic recording devices. This is because various physical properties, including optical, electrical, mechanical, and magnetic properties of nanocrystalline materials can be drastically controlled by changing the synthesis conditions [1-7]. In this viewpoint, one of the most significant features of femtosecond (fs) lasers is direct three-dimensional (3D) processing method [8, 9]. However, studies on space-selective modification of magnetic nanocrystalline materials by fs laser irradiation have been rarely reported. Generally, ultra-short pulse lasers have been utilized for sensing the fast dynamics of magnetic transitions. In such systems, magnetic transitions or changes are transient and relaxed rapidly when the excitation light is turned off [10, 11]. However, some groups have exceptionally observed persistent magnetic phase transitions caused by fs-laser irradiation [12, 13]. In these cases, structural change is essential for achieving a persistent change in the magnetism. In our previous study, we achieved enhancement of magnetization in localized area inside a Fe-oxide-doped transparent paramagnetic glasses by a fs-laser irradiation. This magnetic transition presumably originates from a precipitation of ferrimagnetic Fe_3O_4 nanoparticles, that

occurs as a result of photoreduction of Fe^{3+} ions and crystallization by subsequent anneal process [14]. The laser processing technology has the potential to be used for patterning ferromagnetic materials. In order to develop this technique for application to 3D high-density magnetic recording devices or magneto-optical microdevices, we have tried to crystalize different functional crystals such as magnetic and plasmonic nanoparticles. In this paper, we have fabricated a glasses doped with Au ions and Fe ions and investigated the effect of fs-laser irradiation on magnetic and optical properties.

2. Experimental procedures

Soda lime silicate glass co-doped with Au and Fe-oxide was used in this study. Its composition was $0.01HAuCl_4 \cdot 0.05Fe_2O_3 \cdot 70SiO_2 \cdot 20Na_2O \cdot 10CaO$ (mol/%). We also doped the glass with 0.1 mol% Al to reduce the Fe^{3+} ion effectively. Reagent-grade SiO_2, Na_2CO_3, $CaCO_3$, $HAuCl_4$, Fe_2O_3 (hematite), and Al were used as starting materials. A mixture of these powders was melted in a platinum crucible at 1550 °C for 1 h in air. The melt was then quenched into a transparent glass by casting it onto a stainless-steel plate at room temperature. The polished glass samples with the thickness of about 3 mm were used.

We utilized a near-infrared fs laser (Clark-MXR, CPA-2001; wavelength: 775 nm; repetition rate: 1 kHz; pulse widths: 150 fs (full width at half maximum)). The laser

beam was collimated by a 3-mm-diameter aperture and was focused 1 mm below the glass surface using a ×20 micro-scope objective with a numerical aperture of 0.46. The laser beam had an average power of 20 mW and the beam was focused to produce a 2.7-µm-diameter spot. The sam-ples were placed horizontally on a PC-controlled *XY* trans-lation stage and translated in the *X* direction at a scan speed of 1000 µm/s. Laser-irradiated lines were repeatedly scanned with a pitch of 5 µm in the *Y* direction, producing a square irradiated area with 4-mm-long sides. After the fs-laser irradiation, the glass samples were annealed at 450 ºC for 30 minutes and additionally 30 and 60 minutes (totally 60 and 90 minutes). For comparison, we also annealed a non-irradiated glass sample at 450 ºC and 550 ºC. The ab-sorption spectra of glass samples were measured using a spectrophotometer (JASCO V-570). All magnetic meas-urements were performed using a superconducting quan-tum interference device (SQUID) magnetometer (Quantum Design, MPMS-XL).

3. Results and discussions

3.1 Optical properties

As a preliminary experiment, the glass samples were annealed at 450 and 550 ºC without fs-laser irradiation. Figure 1 shows the absorption spectra of the as-prepared sample and those annealed at each temperature for 30 min. The photographs for each sample were exhibited in the inset. The as-prepared glass sample is highly transparent at visible wavelengths, i.e., wavelengths longer than 340 nm (black curve). This high transparency of glass doped with transition metal Fe ions is ascribed to the small absorption cross section of trivalent Fe ions, which is due to all *d-d* transitions being spin forbidden in a high-spin configura-tion. For the sample after anneal at 450 ºC (red dotted curve), the absorption spectrum is almost equivalent to that for the as-prepared glass sample. In appearance, the optical transparency was maintained in this sample. In the case of the higher temperature anneal (red solid curve), however, we found a distinct absorption peak at around 514 nm, which is due to a red coloration over the whole sample. This change originates from the precipitation of Au nano-particles, which was generated as a result of reduction of Au^{3+} ions and oxidation of Al atoms. Au^{3+} ions received three electrons from Al atoms, at the same time the reduced Au atoms easily aggregated and became nano-sized parti-cles during the high temperature annealing [15, 16]. In other words, single anneal process at the lower temperature (450 ºC) does not cause reduction of Au^{3+} ions, even in the presence of Al atoms.

Absorption spectra were measured for the laser-irradiated and annealed glass samples. Figure 2 displays the difference in spectra between the as-prepared and the each sample. The inset shows photographs of the laser-irradiated sample and that annealed at 450 ºC for 90 min. As can be seen from the top and side-view of the laser-irradiated sample, the laser beam was focused on the local-ized region, which turned brown. This color change is at-tributed to the broad absorption peaks at about 430 and 620 nm in spectrum (a). These absorptions are due to hole-trap centers (e.g., HC_1 and HC_2) at nonbridging oxygens. HC_1 and HC_2 are holes trapped at the nonbridging oxygen in the
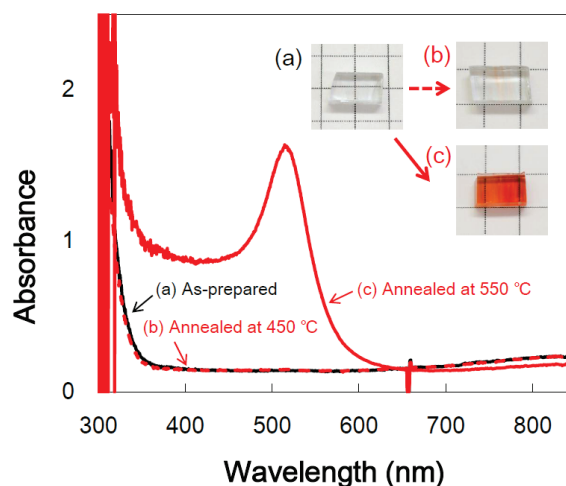
Fig. 1 Optical absorption spectra of as-prepared glass sample (black curve) and that annealed at 450 ºC (red dotted curve) and at 550 ºC (red solid curve) without fs-laser irradiation. The inset shows photographs of the sam-ples.
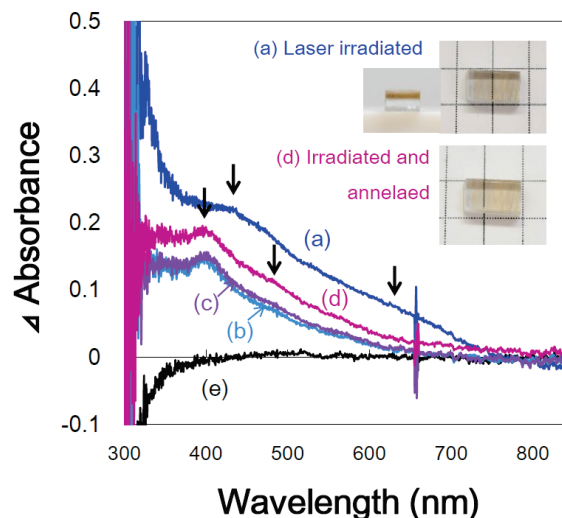
Fig. 2 Difference spectra in absorption spectra between as-prepared and fs-laser irradiated glass samples; the ir-radiated (a), the irradiated and annealed at 450 ºC for 30 min (b), that for 60 min (c), that for 90 min, and only annealed at 450 ºC for 30 min (e). The inset shows photographs of the samples.

SiO_4 polyhedron with two and three nonbridging oxygens, respectively [6, 17, 18]. Free electrons were driven out from the 2*p* orbital of the nonbridging oxygen due to the multiphoton absorption of the incident photons. In the pre-sent case, the doped Al atoms supply electrons to the holes centers on the nonbridging oxygens and form covalent bonds with the oxygens, leading that the free electrons from the oxygens become slightly stable. Hence, Au^{3+} ions would be easily reduced into atomic state by trapping these free electrons. By the following anneal process, the Au atoms agglomerate and Au nanoparticles will be crystalized. In the spectrum for the irradiated and annealed sample (b), the peaks due to hole-trap centers disappeared and another broad absorption peak can be observed at about 485 nm, which is presumably due to localized surface plasmon ab-sorption of the Au nanoparticles. The peak shift from 514 nm suggests that the precipitated Au nanoparticles are

much smaller than those obtained by the annealing at 550 ºC. As increasing the annealing time, the absorption peaks become more intense, indicating the increase in the number of Au nanoparticles (see spectra (c) and (d)). In the meanwhile, a small absorption band was also observed at around 400 nm, the origin of which is unclear. The optical modification has not been definitely induced by the single anneal process at the same temperature, ~ 450 ºC (spectrum (e)).

In our previous paper, we investigated an effect of fs-laser irradiation of Fe^{3+}-doped glass on the optical and magnetic properties [14]. Some Fe^{3+} ions, which disperse in the irradiated region, successfully trap the free electrons and can be reduced to the lower valence state, such as Fe^{2+} [19]. Therefore, a similar phenomenon, namely, reduction of Fe^{3+} ions, is expected to occur also in the present case. As mentioned in our previous paper, reduction of Fe^{3+} induced no change in absorption spectra.

3.2 Magnetic properties

To estimate the change of magnetic properties, we measured the external magnetic field dependences of the magnetization at room temperature. The inset of Fig. 3 shows raw magnetization data for as-prepared sample (black circles), irradiated sample (blue closed circles), and irradiated and annealed samples (blue open symbols). The as-prepared sample had a very low saturation magnetization, M_s, indicating that the sample behaves as a paramagnet at room temperature, because magnetic interactions between Fe ions that are highly dispersed in the glass are significantly weak. Hence, the negligible contribution to the M_s is presumably due to the local magnetic interaction between slightly aggregated Fe ions. On the other hand, the irradiated and annealed samples have relatively higher magnetization compared to the as-prepared sample. Since the ferromagnetic contributions are saturated at high magnetic fields, the negative gradient of the linear diamagnetic component due to the non-magnetic glass matrix can be subtracted as a background. And then, the difference in the magnetization after background subtraction between as-prepared and the other samples are plotted in the main flame of Fig. 3. For comparison, those between the as-prepared and the only annealed samples were also shown (red symbols). The increase in M_s for the irradiated and annealed samples is much larger than that for the annealed sample, which suggests that the fs-laser irradiation is necessary to enhance the magnetization. As is well known, a focused fs laser beam does not affect areas far from the focal point. It is thus reasonable to assume that the change in the magnetization is restricted to the irradiated region. Our previous paper has reported that the precipitation of ferrimagnetic Fe_3O_4 nanoparticles induced by fs-laser irradiation and post anneal process is a possible origin of the enhancement of magnetization. Assuming that the magnetic property of the glass is independent of the other dopants, Al and Au ion, a similar situation will be applied to the present case. Figure 4(a) shows temperature dependences of zero-field-cooled (ZFC) and field-cooled (FC) magnetizations, M_{ZFC} and M_{FC} measured at a dc magnetic field of 500 Oe for the as-prepared and the laser-irradiated samples. While the as-prepared glass is almost completely paramagnetic even at low temperature, the M_{ZFC} deviates from the M_{FC} below room temperature in the case of the irradiated
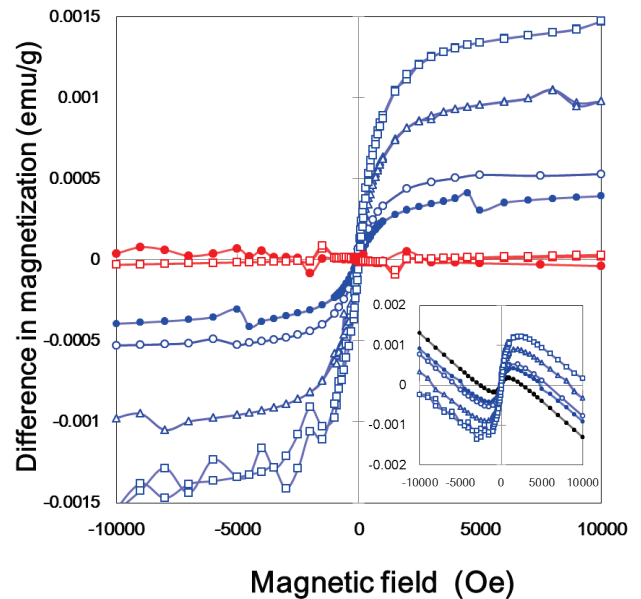
Fig. 3 Inset shows external magnetic field dependences of magnetization at room temperature for the as-prepared (black ●), the irradiated (blue ●), the irradiated and annealed at 450 ºC for 30 min (blue ○), that for 60 min (blue △), that for 90 min (blue □). Main plot shows difference in magnetization between the as-prepared and each sample. For comparison, the only annealed samples at 450 ºC (red ●) and 550 ºC (red □) are also shown.
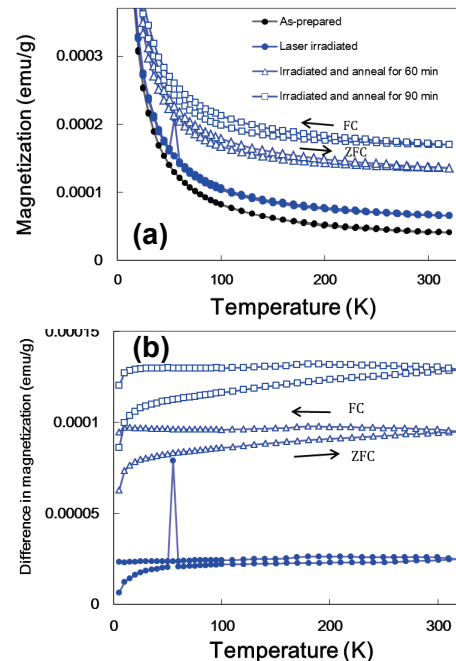
Fig. 4 (a) Temperature dependences of magnetization under an external field of 500 Oe for the as-prepared (black ●), the irradiated (blue ●), the irradiated and annealed for 60 min (blue △), and that for 90 min (blue □). (b) Difference in magnetization between the as-prepared and each sample.

samples. The differences in magnetization between as-prepared and the laser-irradiated samples as a function of temperature are also presented in Fig. 4(b). The irradiated and annealed sample exhibits superparamagnetic blocking above room temperature, which is typically observed in

ferromagnetic nanoparticles with interparticle dipole interactions [11, 20]. It should be noted that the broad and prolonged blocking phenomenon stems from an inhomogeneous dispersion of nanoparticles. In addition, the enhanced magnetization curve for the irradiated and annealed sample has a small coercive field of ~40 Oe, which also implies that high magnetization originates from ferrimagnetic Fe_3O_4 nanoparticles.

The M_s measured for the laser irradiated and annealed glass (90 min) is 3.7 times as high as that for the as-prepared glass. Taking it into account that about 24 % of bulk sample is colored and changes in magnetization, however, an enhancement factor in M_s can be estimated to be 12 at least. In the case the annealing for 60 min, the factor is calculated to be 9.1. This value is almost equivalent to the case of the Fe-singly-doped glass in our previous paper. It should be mentioned that the actual magnetization enhancement could be much greater if the region in which ferrimagnetic nanoparticles crystalized was underestimated. At present, it is impossible to perform an accurate estimation because the change of magnetism is presumably spatially inhomogeneous. The intensity of the focused fs-laser beam decreases with distance from the focal point. Therefore, the spatial density of Fe_3O_4 nanocrystals will vary from area to area depending on the beam intensity distribution.

3.3 Nanostructures

In order to investigate the nanostructure induced by fs-laser in the glass, direct observations were performed using TEM. A plan-view TEM sample was fabricated by an Ar milling process. Figure 5 shows bright field TEM images for the irradiated and annealed glass sample. We have found two kinds of nanoparticles. One (Fig. 5(a)) is 5 to10 nm dark contrasted nanoparticles, which is presumably metallic Au nanoparticles with localized surface plasmon resonance, although a composition analysis has not been carried out yet. The other (Fig.5(b)) is 5 to 18 nm crystalline phase, which indicates a spinel-oxide typed diffraction pattern shown in Fig. 5(c). As discussed before, trivalent Fe ions distributed at around the focal position of the focused laser beam are locally and partly reduced to divalent ions. During the laser irradiation with a fs laser, atomic diffusion of Fe ions occurs due to the heat gradient generated near the focal point [21], resulting in locally Fe-high-density regions. In this case, Fe-oxide phase would be easily crystallized by external thermal stimulation, such as low temperature annealing. Therefore, it is speculated that the possibly crystalized spinel phase is ferrimagnetic Fe_3O_4 which is the most stable crystalline phase in the mixed valence states of Fe ions. Measurements of complementary experiments such as nano-beam diffraction or composition analysis were remaining at present.

4. Conclusions

We demonstrated spatially selective control of optical property and magnetism by focusing an infrared fs laser beam inside transparent Au- and Fe-doped glasses at room temperature and subsequent annealing at 450 ºC. The irradiated area turns brown after laser irradiation and then
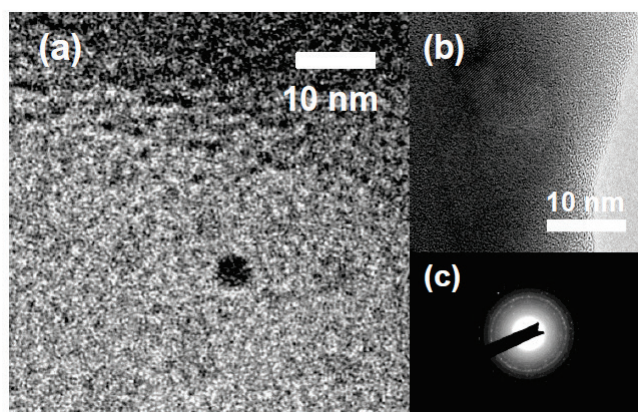
Fig. 5 (a) (b) bright field TEM image for the irradiated and annealed glass sample. (c) Electron-beam-diffraction pattern for the sample.

slightly fades after annealing. The absorption after irradiation is attributed to the formation of hole-trap centers and the generated free electrons locally reduces not only Fe^{3+} ions to Fe^{2+} ions but also Au ions to Au atoms, resulting in localized surface plasmon absorption of Au nanoparticles. The irradiated and annealed glass sample had a higher saturation magnetization than the as-prepared glass, which is due to a ferrimagnetic phase consisting of spinel Fe_3O_4 precipitated and grown by annealing. Nucleation and growth of nanocrystalline phase is confined in local regions with high Fe concentrations formed by an atomic diffusion of Fe ions as a result of high energy deposition by focused fs laser. In this case, magnetic ordering is limited inside the ferrimagnetic nanoparticles, although the magnetic interactions operate even at room temperature. The enhancement factor of the saturation magnetization is estimated to be as high as 12. These results can be explained in terms of co-precipitation of Au nanoparticles and ferrimagnetic spinel-oxide phase nanoparticles in the focused region of the fs-laser beam, which is supported by TEM observations. In the near future, these kinds of materials are practically applicable to extremely novel devices that combine magneto-optical effect with plasmonics [22, 23].

References
[1] J. Qui, , M. Shirai, T. Nakaya, J. Si, X. Jiang, C. Zhu, and K. Hirao, Appl. Phys. Lett. 81, (2002) 3040. (Journals)
[2] K. Miura, J. Qiu, T. Mitsuyu, K. Hirao, Opt. Lett. 25, (2000) 408. (Journals)
[3] B. Zhu, et al., Opt. Express 15, (2007) 6069. (Journals)
[4] S. Kanehira, K. Miura, K. Fujita, K. Hirao, J. Si, N. Shibata and Y. Ikuhara, Appl. Phys. Lett. 90, (2007) 163110. (Journals)
[5] Q. Zhao, J. Qiu, X. Jiang, C. Zhao, and C. Zhu, J. Appl. Phys. 96, (2004) 7122. (Journals)

[6] K. M. Davis, K. Miura, N. Sugimoto, and K. Hirao, Opt. Lett. 21, (1996) 1729. (Journals)

[7] S. Nakashima, K. Fujita, A. Nakao, K. Tanaka, Y. Shimotsuma, K. Miura and K. Hirao, Appl. Phys. A 94, (2009) 83. (Journals)

[8] K. Miura, J. Qiu, H. Inouye, T. Mitsuyu, K. Hirao, Appl. Phys. Lett. 71, (1997) 3329. (Journals)

[9] Y. Cheng, K. Sugioka, K. Midorikawa, M. Masuda, K. Toyoda, M. Kawachi, and K. Shihoyama, Opt. Lett. 28, (2003) 1144. (Journals)

[10] M. Rini, A. Cavalleri, R. W. Schoenlein, R. López, L. C. Feldman, R. F. Haglund, Jr., L. A. Boatner and T. E. Haynes, Opt. Lett. 30, (2005) 558. (Journals)

[11] S. Iwai, S. Tanaka, K. Fujinuma, H. Kishida, H. Okamoto, and Y. Tokura, Phys. Rev. Lett. 88, (2002) 057402. (Journals)

[12] M. Matsubara, Y. Okimoto, T. Ogasawara, S. Iwai, Y. Tomioka, H. Okamoto, and Y. Tokura, Phys. Rev. B 77, (2008) 094410. (Journals)

[13] J. H. Kim, J. Kim, S. U. Lim, C. K. Kim, C. S. Yoon1, G. J. Lee, and Y. P. Lee, J. Appl. Phys. 99, (2006) 08G311. (Journals)

[14] S. Nakashima, K. Sugioka, and K. Midorikawa, Appl. Phys. A, in press (2011). (Journals)

[15] X. Hu, Q. Zhao, X. Jiang, C. Zhu, J. Qiu, Sol. State Comm. 138, (2006) 43. (Journals)

[16] S. Qu, Y. Zhang, H. Li, J. Qiu, C. Zhu, Opt. Materials 29, (2006) 259. (Journals)

[17] A. Bishay, J. Non-Cryst. Solids 3, (1970) 54. (Journals)

[18] J. Qiu, X. Jiang, Q. Zhao, C. Zhu, H. Inoue, J. Si, and K. Hirao, Opt. Lett. 29, (2004) 370. (Journals)

[19] J. Qiu, C. Zhu, T. Nakaya, J. Si, F. Ogura, K. Kojima, and K. Hirao, Appl. Phys. Lett. 79, (2001) 3567. (Journals)

[20] S. Nakashima, K. Fujita, K. Tanaka, and K. Hirao, J. Phys.: Condensed Matter 17, (2005) 137. (Journals)

[21] K. Miura, K. Hirao, Y. Shimotsuma, M. Sakakura, and S. Kanehira, Appl. Phys. A 93, (2008) 183. (Journals)

[22] P. K. Jain, Y. Xiao, R. Walsworth, and A. E. Cohen, Nano lett. 9, (2009) 1644. (Journals)

[23] L. Wang, K. Yang, C. Clavero, A. J. Nelson, K. J. Carroll, E. E. Carpenteer, and R. A. Lukaszew, J. Appl. Phys. 107, (2010) 09B303. (Journals)